Article

J. Biol. Regul. Homeost. Agents. 2024; 38(5): 4089–4097
https://doi.org/10.23812/j.biol.regul.homeost.agents.20243805.324

Emodin Reduces Neuroinflammation in Rats with Acute Severe Craniocerebral Injury

Yan Shen[1,†], Xiahong Tang[1,†], Xiaoyan Zhang[1], Jiawei Zhang[2,*]

[1]Department of Intensive Care Unit, Tongxiang First People's Hospital, 314500 Tongxiang, Zhejiang, China
[2]Department of Neurosurgery, Tongxiang First People's Hospital, 314500 Tongxiang, Zhejiang, China
*Correspondence: zjw594902170@163.com (Jiawei Zhang)
[†]These authors contributed equally.
Published: 1 May 2024

Background: Acute severe craniocerebral injury (ASBI) is a leading cause of morbidity and mortality following trauma. Emodin has demonstrated a range of pharmacological effects, including anti-inflammatory and antioxidant properties. This study sought to investigate the effect of emodin on ASBI in rats and to elucidate its potential mechanisms.
Methods: Thirty sprague-dawley (SD) rats were randomly assigned into five subgroups: the sham subgroup, the model subgroup, the low-dose emodin subgroup, the middle-dose subgroup, and the high-dose subgroup. Initially, we recorded the grip traction time and neurobehavioral scoring in each subgroup. Moreover, pathological injury in brain tissue was observed using hematoxylin-eosin (H&E) staining. Immunohistochemical staining was utilized to evaluate the levels of positive glial fibrillary acidic protein (GFAP) and ionized calcium-binding adapter molecule 1 (Iba1). Furthermore, the levels of cytokines were assessed using biochemical assays. The levels of reactive oxygen species (ROS) in the brain tissue were determined using a 2′,7′-dichlorodihydrofluorescein diacetate (DCFH-DA) probe. Additionally, the mRNA levels of inducible nitric oxide synthase (iNOS) and p38 mitogen-activated protein kinase (p38 MAPK) were evaluated employing quantitative real-time polymerase chain reaction (qRT-PCR). Heat shock proteins 70 (HSP70), B cell lymphoma-2 (Bcl-2), Bcl-2 associated X-protein (Bax), NOD-like receptor (NLR) family pyrin domain-containing protein 3 (NLRP3), caspase-1, iNOS, phosphorylated-p38 MAPK (p-p38 MAPK), p38 MAPK levels in the brain tissue were examined utilizing Western blot analysis.
Results: Emodin treatment significantly improved the neurobehavioral and pathological damage of brain tissue in ASBI rats. HSP70, Bcl-2, glutathione (GSH), and superoxide dismutase (SOD) levels were substantially elevated in the brain tissue of the emodin subgroup. Conversely, emodin treatment reduced the levels of Bax, NLRP3, caspase-1, malondialdehyde (MDA), nitric oxide (NO), and ROS. Furthermore, serum levels of tumor necrosis factor (TNF)-α, interleukin (IL)-1β, interferon-γ (IFN-γ), and IL-6 were significantly reduced in the emodin subgroup compared to the model subgroup ($p < 0.05$). Additionally, iNOS mRNA and protein levels were reduced in the brain tissue of the emodin subgroup compared to the model subgroup ($p < 0.05$). Similarly, the p-p38 MAPK protein concentrations were also alleviated in the brain tissue of the emodin subgroup compared to the model subgroup ($p < 0.05$).
Conclusion: Emodin enhances motor function recovery, mitigates apoptosis and neuroinflammation, and reduces oxidative stress in ASBI rats, potentially through the p38 MAPK signaling pathway.

Keywords: emodin; acute severe craniocerebral injury; p38 MAPK signaling pathway; inflammatory concentration; oxidative stress

Introduction

Acute severe craniocerebral injury (ASBI) is a major contributor to disability and mortality around the world. ASBI often results from external mechanical forces, comprising head collisions, blows, or jolts, as well as penetrating head injuries, leading to several intracranial complications like hemorrhage, bruises, lacerations, and focal and diffuse injuries [1,2]. ASBI can lead to neurological impairment, behavioral changes, and cognitive dysfunction, immensely impacting patients' lives. Although the research on the recovery strategy of ASBI has made progress, useful therapy plans are needed [3]. Overactivation of neuroinflammatory response, mediated through microglia activation, plays a crucial role in secondary brain injury and is essential in ASBI [4]. Thus, it is imperative to identify effective drugs to alleviate the secondary injury induced by nerve inflammation.

Emodin, a natural anthraquinone derivative extracted from Chinese herbal medicine, including *Rheum palmatum L*, *Polygonum multiflorum*, and *Polygonum cuspidatum*, exhibits a wide range of pharmacological properties, such as anticancer, anti-inflammatory, antioxidant, and antibacterial effects [5–7]. Emodin has a neuroprotective outcome and can reduce inflammatory response and oxidative stress induced by ischemia-reperfusion [8]. Emodin effectively

Journal of
BIOLOGICAL REGULATORS
and Homeostatic Agents

reduces infarct size, alleviates nerve injury symptoms, and reduces neurological impairment scores in rat with cerebral artery occlusion [9]. However, the precise influence of emodin on ASBI and its underlying mechanism are unclear.

The p38 mitogen-activated protein kinase (p38 MAPK) is widely known for its role in modulating inflammation, apoptosis, and cell differentiation. Previous study [10] has demonstrated that in instances of stress-induced neuronal dysfunction, p38 MAPK transduces signals from cell membranes to the nucleus, thereby regulating gene expression to cope with environmental changes, which is considered the basis of brain injury. Furthermore, research has indicated that activating the p38 MAPK signaling pathway can lead to the activation of rat microglia, elevated levels of proinflammatory cytokines, neuronal degeneration, and disturbance of behavior. Moreover, it has been shown that emodin targets p38 MAPK, leading to a reduction in the expression levels of proinflammatory cytokines and chemokines in the liver of hepatitis mice by inhibiting the p38 MAPK signaling pathway.

Therefore, this study aims to explore the impact of emodin on ASBI in rats, focusing on neuroinflammation and oxidative stress, and investigate the potential role of the p38 MAPK signal pathway in regulating the effects of emodin on ASBI rats.

Materials and Methods

Animal Assay

SPF-grade male sprague-dawley (SD) rats (n = 30), weighing 200–220 g, were obtained from Beijing Baosco Biomedical Technology Co., Ltd., Beijing, China [11]. The rats were anesthetized using intraperitoneal injection of 3% pentobarbital sodium (50 mg/kg, P3761, Sigma-Aldrich, St. Louis, MO, USA), following the previously described method for modeling. The top of the skull was disinfected and depilated, and a midline incision on the skull was made without disrupting the dura mater. A 5-mm craniotomy was conducted through the skull, positioned 2 mm caudal to the left coronal suture and 2 mm from the midline without destroying the dura matter. A percussion device with a diameter of 4.5 mm and a weight of 40 g was utilized from a height of 20 cm to hit the dura mater and induce craniocerebral injury. After local hemostasis, the skin was disinfected and sutured. After this, the rats were exposed to emodin (E7881, Sigma-Aldrich, St. Louis, MO, USA). The rats were stochastically divided into five subgroups: the sham subgroup, the model subgroup, the emodin low-dose (10 mg/kg) subgroup, the emodin middle-dose (20 mg/kg) subgroup, and the emodin high-dose (40 mg/kg) subgroup, each comprising 6 rats. Except for the sham subgroup, all other 4 subgroups underwent the above method to establish the ASBI model. One day after successful modeling, each subgroup received corresponding treatment. The sham subgroup and the model subgroup were injected with an equal volume of normal saline, while the emodin subgroup was administered with different concentrations of emodin once a day for 7 days.

Grip Traction Assay

On the 7th day of administration, a steel wire rope measuring 1 mm in diameter and 60 cm in length was positioned about 40 cm above the ground, with a foam pad placed beneath it to avoid any falls [12]. The rat's forepaws were placed on the steel wire rope, and the time from release to fall was recorded. The scoring criteria were as follows: 0 point, unable to grasp; 1 point, grasping $\leq$10 s; 2 points, 10 $<$ 20 s; 3 points, 20 $<$ 30 s; 4 points: 30 $<$ 60 s; 5 points, 60 $<$ 90 s; 6 points, 90 $<$ 120 s.

Neurobehavioral Score

The neurobehavioral changes of rats within each subgroup were observed and scored. The observation included changes in the auricle reflex, tail flick reflex, righting reflex, corneal reflex, and escape reflex. The scores of no reflex, lessened reflex (lack of corresponding reflex within 10 seconds), normal reflex and neurobehavioral total score of each rat were 0, 1, 2 and 10, respectively.

Hematoxylin-eosin (H&E) Staining

Once the brains were collected, the cerebellum and its covering membranes were excised. The brain tissue sections (4 μm thick) were prepared using routine procedure and routinely dewaxed to water. Subsequently, hematoxylin-eosin staining (G1120, Solarbio, Beijing, China) was used to observe pathological changes in brain tissue under a microscope (BX5, Olympus, Tokyo, Japan).

Immunohistochemical (IHC) Staining

After the completion of the grip traction test and neurobehavioral score assessment, the rats were killed through intraperitoneal injection of excessive pentobarbital sodium (200 mg/kg). The rat's heart was washed with 0.9% NaCl solution (ST341, Beyotime Biotechnology, Shanghai, China) to remove blood, and then perfused with 4% paraformaldehyde (MM1504, Maokang Biotechnology Co., Ltd., Shanghai, China) until the limbs were stiff. The brain was excised through craniotomy, fixed in 4% paraformaldehyde, and temporarily stored at 4 °C. Brain tissue sections (3 μm thick) were prepared using the routine procedure and dewaxed to water. After this, 1 mM Tris-EDTA buffer (G1203, Servicebio, Wuhan, China) was added to repair tissue sections for 18 minutes under high pressure (125 °C, 103 kPa), followed by soaking in 3% H_2O_2 (MM0750, Maokang Biotechnology Co., Ltd., Shanghai, China) to block endogenous peroxidase activity for 10 minutes. After washing, the slices were sealed in 10% goat serum (SL038, Solarbio, Beijing, China) for 30 minutes. The tissue section then underwent overnight in-

cubation with primary antibodies against ionized calcium-binding adapter molecule 1 (Iba1, 1:500, ab5076, Abcam, Cambridge, UK) and glial fibrillary acidic protein (GFAP, 1:1000, ab4674, Abcam, Cambridge, UK) at 4 °C. Subsequently, these sections were treated with 50 µL of sheep anti-mouse IgG second antibody (KIT-5020, Mxb Biotechnologies, Fuzhou, China) and incubated for 1 hour. After staining with 3-3-diaminobenzidine (DAB, DAB-1031, Mxb Biotechnologies, Fuzhou, China), hematoxylin was applied for 3 minutes, followed by treatment with 1% hydrochloric acid (E484, Amresco, Solon, OH, USA) and alcohol for differentiation and washing to eliminate the dye. After ethanol dehydration, xylene was employed to make the sections transparent, followed by sealing with neutral resin. The stained tissue sections were observed, and images were captured using a microscope (DM1000, Leica Microsystems, Wetzlar, Hessen, Germany).

Biochemical Testing

After completing the grip traction experiment and neurobehavioral scoring, the rats were anesthetized, and blood samples were collected from the abdominal aorta. The blood sample was centrifuged, and the supernatant was temporarily stored at –20 °C. The levels of tumor necrosis factor (TNF)-α (H052), interleukin (IL)-1β (H002), interferon-γ (IFN-γ, H025), and IL-6 (H007) in serum were assessed using corresponding enzyme linked immunosorbent assay (ELISA) kits. Additionally, malondialdehyde (MDA), nitric oxide (NO), glutathione (GSH), and superoxide dismutase (SOD) levels in brain tissues were determined using MDA assay kits (A003), NO assay kits (A012), GSH assay kits (A006), and SOD assay kits (A001), respectively. These kits were obtained from Nanjing Jiancheng Bioengineering Institute (Nanjing, China).

2′,7′-dichlorodihydrofluorescein Diacetate (DCFH-DA) Probe Detection

The rat brain tissue was chopped and digested with trypsin, then filtered with a 200-micron nylon mesh filter. Following centrifugation at 400 g for 5 minutes, the supernatant was discarded, and the pellets were resuspended in PBS. The suspension was gently blown repeatedly, resulting in a 1×10^8 L^{-1} single-cell suspension. The single-cell suspension of rat brain tissue was incubated with DCFH-DA (35845, Sigma-Aldrich, St. Louis, MO, USA) at 37 °C for 30 minutes, following the instructions provided by the kit. After incubation, the cells were rinsed twice with PBS, and a fluorescence enzyme marker (Thermo Scientific, Varioskan Flash, Waltham, MA, USA) was utilized to examine fluorescence intensity, with excitation at a wavelength of 485 nm and emission at 530 nm.

Quantitative Real-time Polymerase Chain Reaction (qRT-PCR)

Total RNA was extracted from brain tissue using Trizol (15596026, Ambion, Carlsbad, CA, USA), and cDNA was synthesized through reverse transcription. qRT-PCR was performed using a cDNA template. The amplification conditions were set as follows: 95 °C 3 min; 95 °C 5 s, 56 °C 10 s, 72 °C 25 s, a total of 40 cycles. PCR primers were synthesized from Wuhan Tianyi Huayu Gene Technology Co., Ltd. Primer sequences were as follows: inducible nitric oxide synthase (*iNOS*) forward sequence: 5′-AGAGAGATCGGGTTCACA-3′, reverse sequence: 5′-CACAGAACTGAGGGTACA-3′; p38 mitogen-activated protein kinase (*p38 MAPK*) forward sequence: 5′-CTACCCGCAGGAGCTGAACAA-3′, reverse sequence: 5′-AATCATGGACTGAAATGGTCTCCAG-3′; glyceraldehyde-3-phosphate dehydrogenase (*GAPDH*) forward sequence: 5′-CCAGGTGGTCTCCTCTGA-3′, reverse sequence: 5′-GCTGTAGCCAAATCGTTGT-3′. The relative expression levels of the target genes were assessed employing the $2^{-\Delta\Delta Ct}$ method. *GAPDH* served as an internal reference.

Western Blot (WB) Analysis

Total protein was extracted using the RIPA lysis buffer (R0030, Solarbio, Beijing, China) and subsequently quantified utilizing a Bicinchoninic acid kit (PC0020, Solarbio, Beijing, China). 20 µg extracted proteins were isolated and transferred to polyvinylidene fluoride membranes (IPVH00010, Millipore, Bedford, MA, USA). The membrane was blocked in 5% skim milk powder (D8340, Solarbio, Beijing, China) at 4 °C overnight. The following day, the membrane was incubated for 12 hours with primary antibodies against GAPDH (5174, 1:1000, CST, Boston, MA, USA), heat shock proteins 70 (HSP70, ab181606, 1:1000, Abcam, Cambridge, UK), B cell lymphoma-2 (Bcl-2, PAB30041, 1:1000, Bioswamp, Wuhan, China), Bcl-2 associated X-protein (Bax, PAB30040, 1:1000, Bioswamp, Wuhan, China), NOD-like receptor (NLR) family pyrin domain-containing protein 3 (NLRP3) (K004108P, 1:1000, Solarbio, Beijing, China), caspase-1 (K001773P, 1:1000, Solarbio, Beijing, China), iNOS (SAB5700636, 1:1000, Sigma-Aldrich, St. Louis, MO, USA), phosphorylated-p38 MAPK (p-p38 MARK, 4511, 1:1000, CST, Boston, MA, USA), and p38 MAPK (2387, 1:1000, CST, Boston, MA, USA). After this, the membrane underwent incubation with IgG secondary antibody (K1034G-AF594, Solarbio, Beijing, China) for 1 hour. GAPDH was used as an endogenous control.

Statistical Analysis

Statistical analysis was performed using SPSS software (version 22.0, IBM, Armonk, NY, USA). The data were presented as the average and standard deviation (mean $\pm$ SD). Normality was confirmed for all variables utilizing

Journal of
BIOLOGICAL REGULATORS
and Homeostatic Agents

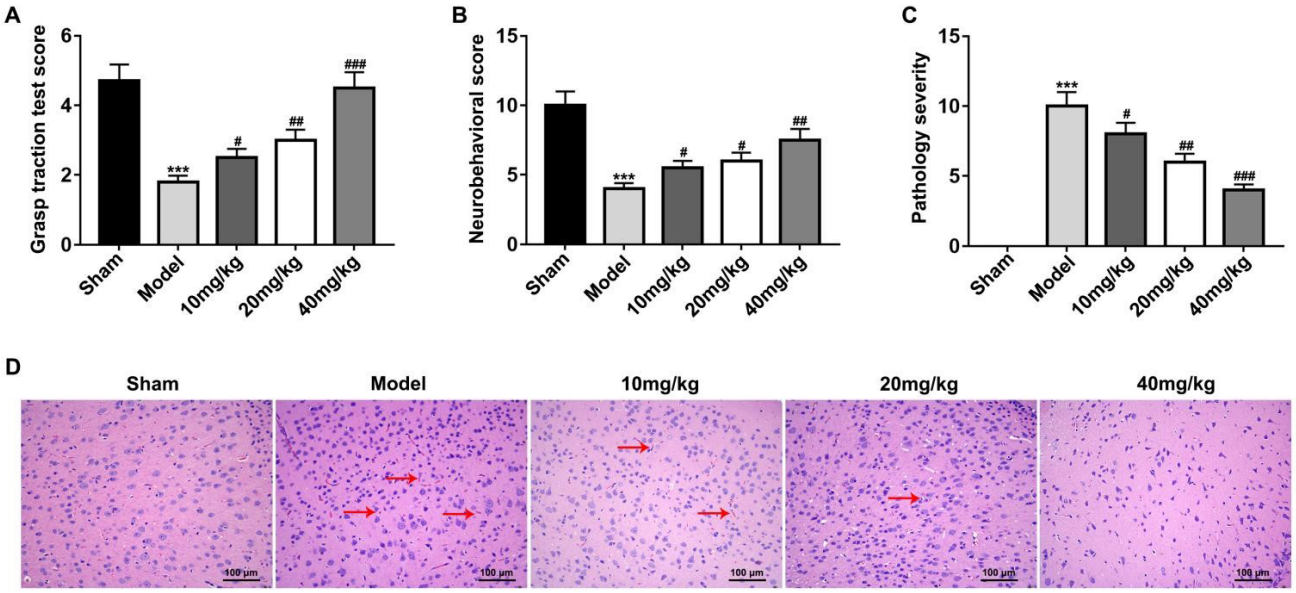

Fig. 1. Neurobehavioral and pathological injury scores in rats. (A) Grip traction experiment. (B) Comparison of neurobehavioral scores in rats. (C,D) The level of pathological injury was observed using the hematoxylin-eosin (H&E) staining (Scale: 100 μm, magnification: 200×). $^{***}p < 0.001$, vs the sham subgroup; $^{\#}p < 0.05$, $^{\#\#}p < 0.01$, $^{\#\#\#}p < 0.001$, vs the model subgroup (n = 3). The red arrow indicates that the atrophied neurons appear red.

histograms and Q–Q plots. Furthermore, subgroup comparisons were conducted through the one-way analysis of variance (ANOVA). A p-value < 0.05 was set as a threshold for statistical significance.

Results

Emodin Ameliorated Neurobehavioral and Pathological Injury in ASBI Rats

We treated the ASBI rat model with different concentrations of emodin to assess its impact on ASBI. The grip traction time and neurobehavioral score were significantly lower in the model subgroup than in the sham subgroup. However, the grip traction time and neurobehavioral score were significantly increased in the emodin subgroup compared to the model subgroup (Fig. 1A,B). Moreover, in the sham subgroup, the brain tissue structure was intact, and the nucleus was normal without swelling. Furthermore, the model subgroup showed a significant increase in neuronal necrosis, glial cell proliferation, and neutrophil infiltration compared to the sham subgroup. While these pathological changes in brain tissue were alleviated in the emodin subgroups, neuronal necrosis, neutrophil infiltration, tissue cavity, and cell edema were evident, particularly in the high-dose emodin subgroup compared to the model subgroup (Fig. 1C,D).

Emodin Inhibited Apoptosis in ASBI Rat Model

The levels of HSP70 and Bcl-2 proteins in the brain tissue of the model subgroup showed a substantial reduction, while the level of Bax protein was significantly elevated compared to the sham subgroup. In contrast, the levels of HSP70 and Bcl-2 proteins in the brain tissue of the emodin subgroup were significantly higher, while the level of Bax protein was lower compared to the model subgroup (Fig. 2A–D). IHC staining revealed that the astrocytes and microglia showed normal morphology and even distribution in the sham operation subgroup. However, in the model subgroup, astrocytes and microglia were substantially activated and clustered, with significantly elevated positive areas of Iba1 and GFAP compared to the sham operation subgroup. Conversely, compared to the model subgroup, the activation of astrocytes and microglia in the emodin subgroup was substantially reduced, accompanied by an alleviation in the positive areas of GFAP and Iba1 (Fig. 2E–G).

Emodin Inhibited Inflammatory Response in ASBI Rat Model

The levels of tumor necrosis factor (TNF)-α, interleukin (IL)-1β, interferon-γ (IFN-γ) and IL-6 were significantly increased in the model subgroup compared to the sham subgroup. Conversely, the levels of these inflammatory factors were substantially alleviated in the emodin subgroup compared to the model subgroup (Fig. 3A–D). Furthermore, the model subgroup exhibited a significant increase in the levels of NLRP3 and caspase-1 proteins, while these proteins showed substantial reduction in the emodin subgroup compared to the model subgroup (Fig. 3E–G).

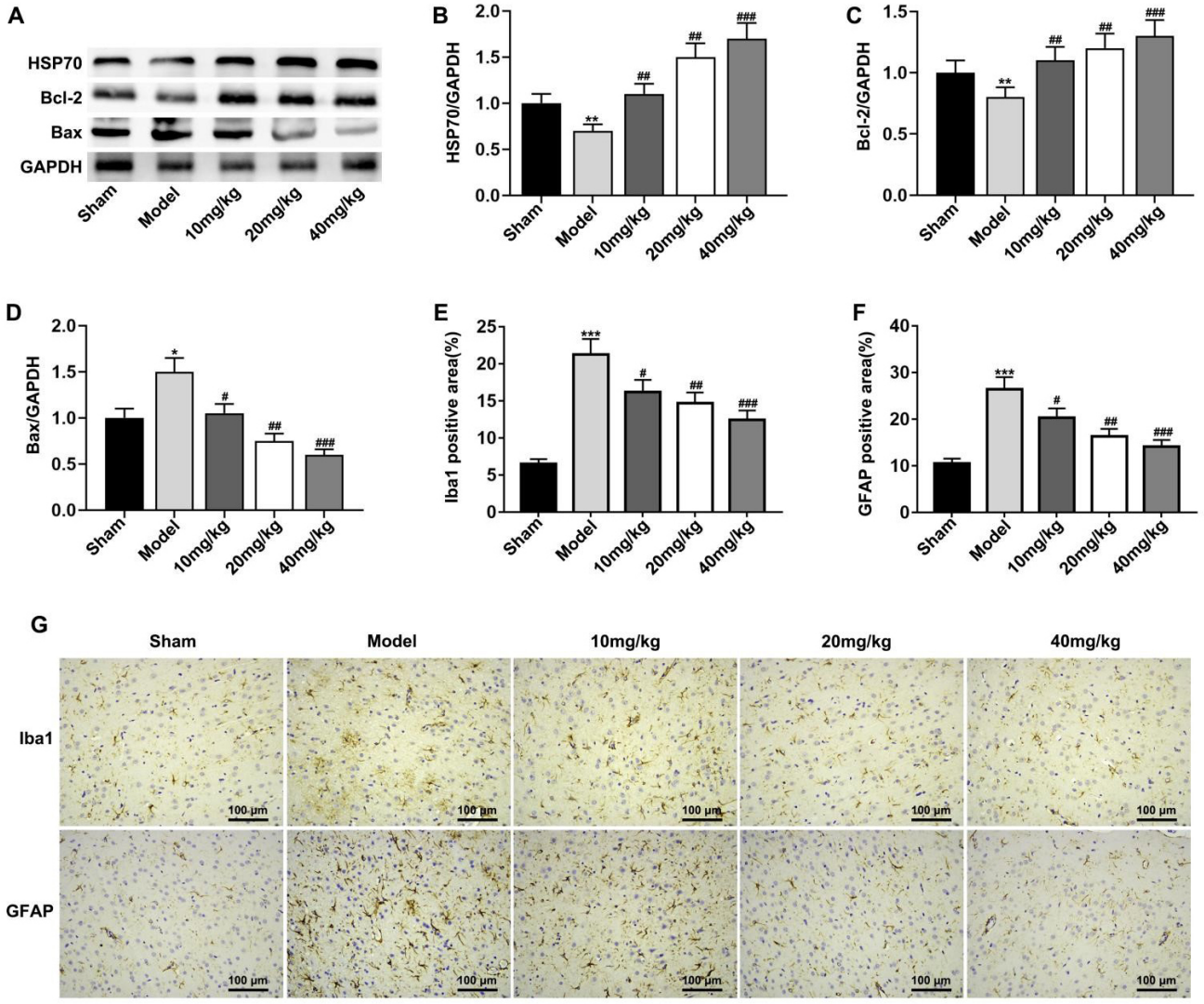

Fig. 2. Emodin inhibited apoptosis in the acute severe craniocerebral injury (ASBI) rat model. (A–D) Heat shock proteins 70 (HSP70), B cell lymphoma-2 (Bcl-2), and Bcl-2 associated X-protein (Bax) levels were assessed using western blot (WB) analysis. (E–G) Ionized calcium-binding adapter molecule 1 (Iba1) and glial fibrillary acidic protein (GFAP) positive area were evaluated using Immunohistochemical (IHC) staining. Scale: 100 μm. $^{*}p < 0.05$, $^{**}p < 0.01$, $^{***}p < 0.001$, vs the sham subgroup. $^{\#}p < 0.05$, $^{\#\#}p < 0.01$, $^{\#\#\#}p < 0.001$, vs the model subgroup. Each experiment was repeated three times. GAPDH, glyceraldehyde-3-phosphate dehydrogenase.

Emodin Inhibited Oxidative Stress Injury in ASBI Rat Model

The levels of MDA and NO were significantly increased in the brain tissue of the model subgroup, while the levels of GSH and SOD were decreased compared to the sham subgroup. Conversely, a substantial reduction was observed in the concentrations of MDA and NO in the emodin subgroup, while GSH and SOD concentrations were elevated in a dose-dependent manner compared to the model subgroup (Fig. 4A–D). The fluorescence results showed that the reactive oxygen species (ROS) concentration in the brain tissue of the model subgroup was significantly higher than that of the sham subgroup, whereas in the emodin subgroup, it was substantially lower than that in the model subgroup in a dose-dependent manner (Fig. 4E,F).

Emodin Inhibited ASBI Mediated by p38 MAPK Signal Pathway

As depicted in Fig. 5, the iNOS mRNA level was substantially increased in the model subgroup compared to the sham subgroup, whereas it was reduced in the emodin subgroup compared to the model subgroup (Fig. 5A). Moreover, the mRNA and protein levels of the p38 MAPK among different subgroups did not show an observable distinction (Fig. 5B,F). Furthermore, the model subgroup exhibited a significant elevation in the levels of iNOS and p-p38 MARK proteins compared to the sham subgroup (Fig. 5C,D). In contrast, their levels were substantially reduced in the emodin subgroup compared to the model subgroup (Fig. 5E).

Journal of
BIOLOGICAL REGULATORS
and Homeostatic Agents

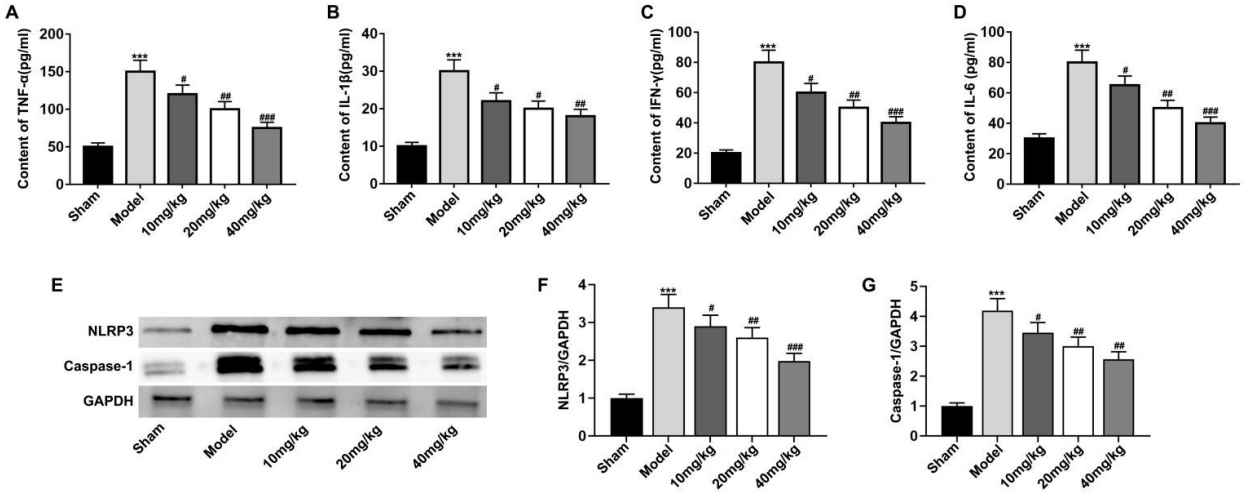

Fig. 3. Emodin inhibited inflammation in the ASBI rat model. (A–D) Enzyme linked immunosorbent assay (ELISA) was used to evaluate the levels of tumor necrosis factor (TNF)-α, interleukin (IL)-1β, interferon-γ (IFN-γ) and IL-6. (E–G) WB analysis was conducted to evaluate the levels of inflammatory proteins NOD-like receptor (NLR) family pyrin domain-containing protein 3 (NLRP3) and caspase-1. $^{***}p < 0.001$, vs the sham subgroup. $^{\#}p < 0.05$, $^{\#\#}p < 0.01$, $^{\#\#\#}p < 0.001$, vs the model subgroup. Each experiment was repeated three times.

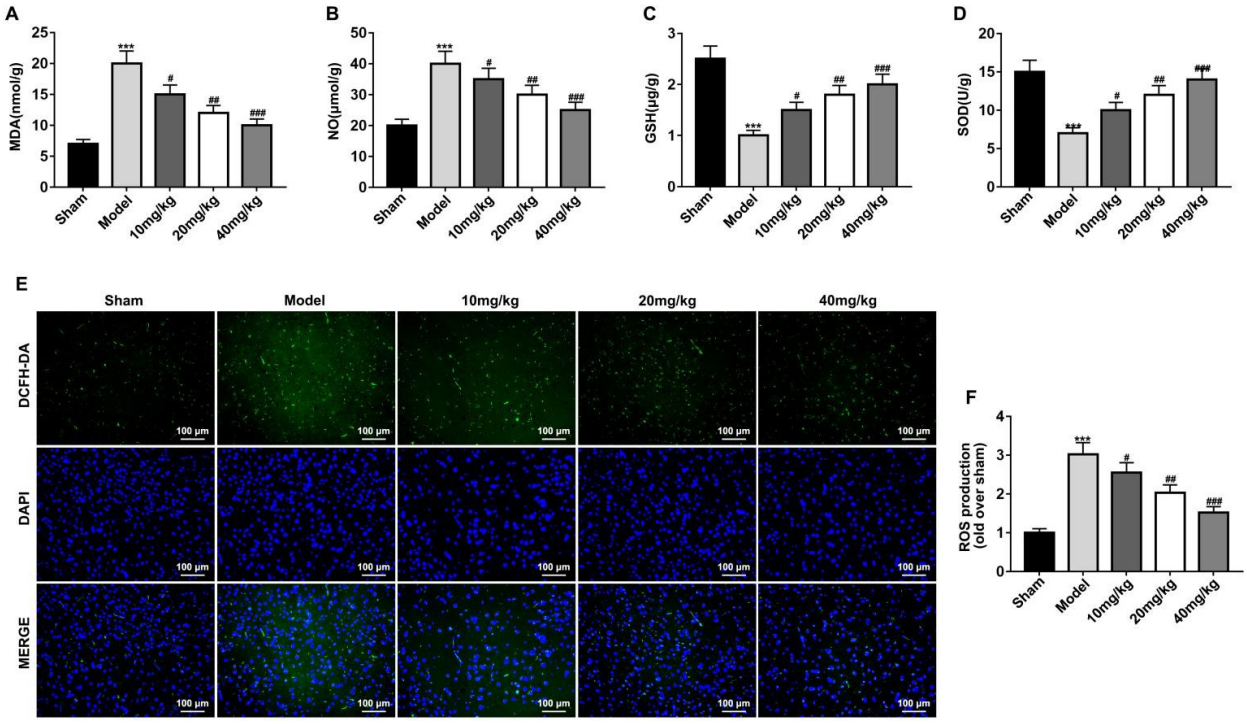

Fig. 4. Emodin inhibited oxidative stress injury in the ASBI rat model. (A–D) The levels of malondialdehyde (MDA), nitric oxide (NO), glutathione (GSH), and superoxide dismutase (SOD) were assessed according to the instructions provided by the kit. (E,F) Reactive oxygen species (ROS) staining. Scale: 100 μm. $^{***}p < 0.001$, vs the sham subgroup. $^{\#}p < 0.05$, $^{\#\#}p < 0.01$, $^{\#\#\#}p < 0.001$, vs the model subgroup. Each experiment was repeated three times. DCFH-DA, 2′,7′-dichlorodihydrofluorescein diacetate; DAPI, 4′6-diamidino-2-phenylindole.

Discussion

The effect of emodin on ASBI was assessed by evaluating its impact on neurobehavioral outcomes and brain pathology in ASBI. The results of the grip traction test and the neurobehavioral scoring showed that emodin extended the grip traction time and increased neurobehavioral scores in model rats compared to the model subgroup.

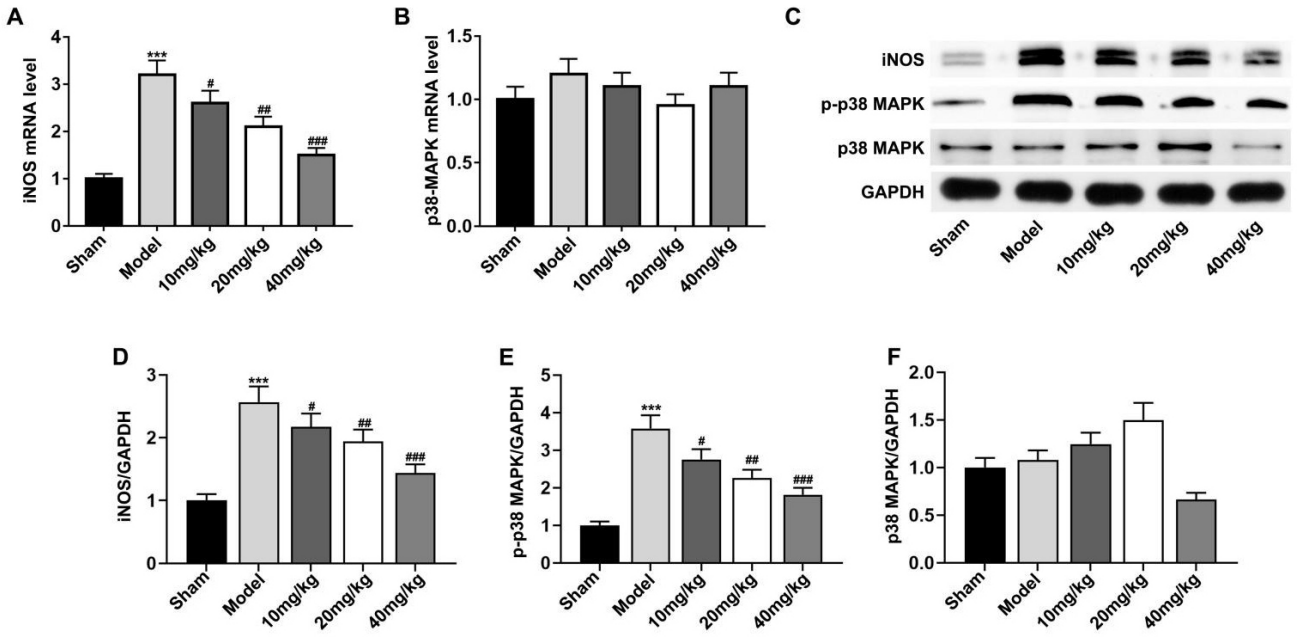

Fig. 5. Emodin inhibited ASBI mediated by the p38 MAPK signal pathway. (A,B) Quantitative real-time polymerase chain reaction (qRT-PCR) was employed to assess the levels of inducible nitric oxide synthase (iNOS) and p38 mitogen-activated protein kinase (p38 MAPK) mRNAs. (C–F) The protein concentrations of iNOS, phosphorylated-p38 MARK (p-p38 MAPK), and p38 MAPK were evaluated using WB analysis. $^{***}p < 0.001$, vs the sham subgroup. $^{\#}p < 0.05$, $^{\#\#}p < 0.01$, $^{\#\#\#}p < 0.001$, vs the model subgroup. Each experiment was repeated three times.

Furthermore, H&E staining indicated that emodin alleviated the pathological changes associated with ASBI. These outcomes suggest that emodin exhibits a protective impact against nerve and brain tissue injury in ASBI rats.

Apoptosis plays a pivotal role in various nervous system diseases. Neuronal apoptosis is found in patients with ASBI based on *in vivo* analysis [13]. In a mouse model of septic encephalopathy, emodin has been found to increase Bcl-2 protein levels while decreasing Bax and cleaved caspase-3 concentrations, indicating a decrease in neuronal apoptosis [14]. HSP70, a stress protein recognized for maintaining its stability, is rapidly induced following mammalian brain injury, displaying a substantial protective impact on brain tissue and potentially participating in the occurrence and development of ASBI [15]. Iba1 is a marker for activated microglia, whose activation mediates severe neurological response and aggravates brain injury [16]. GFAP is expressed explicitly in astrocytes and is one of the extensively studied biomarkers of ASBI patients [17]. After administering different concentrations of emodin, compared with the model subgroup, our study revealed elevated levels of HSP70 and Bcl-2 proteins and reduced levels of Bax proteins in brain tissue. Immunohistochemical staining validated the alleviation in the activation of astrocytes and microglia, and the decrease in the positive area of GFAP and Iba1 in the emodin subgroup.

Neuroinflammation influences the physiological process associated with ASBI [18]. During the early stage of ASBI, resident microglia become activated, and peripheral neutrophils are recruited to the peri-focal cortex. Subsequently, the chemokine signaling pathway facilitates the recruitment and infiltration of immune cells into the damaged cortex. Concurrently, these immune cells release inflammatory cytokines, including TNF-α, IL-1β, and IL-6. Excessive post-traumatic neuroinflammation can lead to secondary brain injury and neuronal death in the peri-focal cortex and hippocampus, thereby exacerbating neurological dysfunction [19]. Activation of NLRP3 inflammasomes leads to the cleavage of caspase-1 precursor form, resulting in the release of IL-1β and IL-18, consequently inducing neuronal degradation [20,21]. The proinflammatory response mediated by NLRP3 inflammasomes plays a crucial role in ASBI [22]. It has been indicated that the levels of TNF-α, IL-1β, IFN-γ, and IL-6 in the serum of ASBI model rats increase. As corroborated, NLRP3 and caspase-1 concentrations in the brain tissue of ASBI model rats were found to be upregulated. After emodin administration, levels of TNF-α, IL-1β, IFN-γ, and IL-6 reduced, along with a decrease in NLRP3 and caspase-1 concentrations. These outcomes suggest that emodin can inhibit neuroinflammation in ASBI.

Mechanical damage in ASBI triggers metabolic and ion imbalances, eventually leading to excessive production of ROS and oxidative stress [23]. Previous studies have demonstrated the antioxidation properties of emodin [24,25]. In our study, we observed that emodin treatment

Journal of
BIOLOGICAL REGULATORS
and Homeostatic Agents

significantly reduced the levels of MDA, NO, and ROS while elevating GSH and SOD concentrations in the brain tissue of ASBI model rats. Thus, it is suggested that emodin can alleviate the oxidative stress in ASBI.

The MAPK pathway plays an essential role in regulating the release of proinflammatory cytokines and apoptosis. MAPK, a family of serine/threonine protein kinases, includes ERK, JNK, and p38. Activation of MAPK leads to the upregulation of caspase-3 and a decrease in Bcl-2, thereby enhancing cell apoptosis [26]. Downregulation of the p38 MAPK pathway can reduce the production of inflammatory cytokines, chemokines, and mediators, as well as the release of nitric oxide, thus inhibiting neuroinflammation in ASBI [27]. This study showed an increase in iNOS mRNA and protein levels, as well as the level of p-p38 MAPK protein, in the brain tissue of the model subgroup. In contrast, emodin treatment reduced the expression levels of iNOS mRNA and protein, as well as the level of p-p38 MAPK protein in the brain tissue of rats. These findings suggest the role of the p38 MAPK signaling pathway in the outcome of emodin in ASBI rats. Additionally, future endeavors will include long-term follow-up studies to assess the persistence of emodin treatment effects and any potential delayed side effects.

Conclusion

In summary, emodin enhances motor function recovery, inhibits apoptosis and neuroinflammation, and alleviates oxidative stress in ASBI rats. Its underlying mechanism is likely linked to the modulation of the p38 MAPK signal pathway. However, this study acknowledges certain limitations. Therefore, future studies should further explore the molecular targets and signaling pathways implicated in emodin's effects, as well as elucidate how these mechanisms interact with the pathological processes of ASBI.

Availability of Data and Materials

The dataset analyzed during the current study are available upon request by contact with the corresponding author.

Author Contributions

YS and XHT contributed to the concept and designed the research study. XHT performed the research. XYZ made data collection and manuscript preparation. JWZ provided help and advice on the data analysis. YS analyzed the data. XHT and XYZ wrote the manuscript. All authors contributed to editorial changes in the manuscript. All authors read and approved the final manuscript. All authors have participated sufficiently in the work and agreed to be accountable for all aspects of the work.

Ethics Approval and Consent to Participate

All experimental protocols were approved by the ethic committee of Beijing Biocisco Biomedical Technology Co., Ltd. (MDL2023-03-22-01), in compliance with the ARRIVE guidelines and carried out in accordance with the U.K. Animals Act.

Acknowledgment

Not applicable.

Funding

This research received no external funding.

Conflict of Interest

The authors declare no conflict of interest.

References

[1] Ghaith HS, Nawar AA, Gabra MD, Abdelrahman ME, Nafady MH, Bahbah EI, *et al*. A Literature Review of Traumatic Brain Injury Biomarkers. Molecular Neurobiology. 2022; 59: 4141–4158.

[2] Wang Z, Wang Z, Wang A, Li J, Wang J, Yuan J, *et al*. The neuroprotective mechanism of sevoflurane in rats with traumatic brain injury via FGF2. Journal of Neuroinflammation. 2022; 19: 51.

[3] van Vliet EA, Ndode-Ekane XE, Lehto LJ, Gorter JA, Andrade P, Aronica E, *et al*. Long-lasting blood-brain barrier dysfunction and neuroinflammation after traumatic brain injury. Neurobiology of Disease. 2020; 145: 105080.

[4] He X, Huang Y, Liu Y, Zhang X, Yue P, Ma X, *et al*. BAY61 3606 attenuates neuroinflammation and neurofunctional damage by inhibiting microglial Mincle/Syk signaling response after traumatic brain injury. International Journal of Molecular Medicine. 2022; 49: 5.

[5] Zou G, Zhang X, Wang L, Li X, Xie T, Zhao J, *et al*. Herb-sourced emodin inhibits angiogenesis of breast cancer by targeting VEGFA transcription. Theranostics. 2020; 10: 6839–6853.

[6] Guo Y, Zhang R, Li W. Emodin in cardiovascular disease: The role and therapeutic potential. Frontiers in Pharmacology. 2022; 13: 1070567.

[7] Zhang Y, Pu W, Bousquenaud M, Cattin S, Zaric J, Sun LK, *et al*. Emodin Inhibits Inflammation, Carcinogenesis, and Cancer Progression in the AOM/DSS Model of Colitis-Associated Intestinal Tumorigenesis. Frontiers in Oncology. 2021; 10: 564674.

[8] Dong X, Wang L, Song G, Cai X, Wang W, Chen J, *et al*. Physcion Protects Rats Against Cerebral Ischemia-Reperfusion Injury via Inhibition of TLR4/NF-kB Signaling Pathway. Drug Design, Development and Therapy. 2021; 15: 277–287.

[9] Lv B, Zheng K, Sun Y, Wu L, Qiao L, Wu Z, *et al*. Network Pharmacology Experiments Show That Emodin Can Exert a Protective Effect on MCAO Rats by Regulating Hif-1α/VEGF-A Signaling. ACS Omega. 2022; 7: 22577–22593.

[10] Zhu W, Li W, Jiang J, Wang D, Mao X, Zhang J, *et al*. Chronic salmon calcitonin exerts an antidepressant effect via modulating the p38 MAPK signaling pathway. Frontiers in Molecular Neuroscience. 2023; 16: 1071327.

[11] Chen X, Chen C, Fan S, Wu S, Yang F, Fang Z, *et al*. Omega-3 polyunsaturated fatty acid attenuates the inflammatory response

by modulating microglia polarization through SIRT1-mediated deacetylation of the HMGB1/NF-κB pathway following experimental traumatic brain injury. Journal of Neuroinflammation. 2018; 15: 116.

[12] Thal SC, Mebmer K, Schmid-Elsaesser R, Zausinger S. Neurological impairment in rats after subarachnoid hemorrhage–a comparison of functional tests. Journal of the Neurological Sciences. 2008; 268: 150–159.

[13] Jiang W, Jin P, Wei W, Jiang W. Apoptosis in cerebrospinal fluid as outcome predictors in severe traumatic brain injury: An observational study. Medicine. 2020; 99: e20922.

[14] Gao LL, Wang ZH, Mu YH, Liu ZL, Pang L. Emodin Promotes Autophagy and Prevents Apoptosis in Sepsis-Associated Encephalopathy through Activating BDNF/TrkB Signaling. Pathobiology: Journal of Immunopathology, Molecular and Cellular Biology. 2022; 89: 135–145.

[15] Zhao J, Wang T, Lv Q, Zhou N. Expression of heat shock protein 70 and Annexin A1 in serum of patients with acutely severe traumatic brain injury. Experimental and Therapeutic Medicine. 2020; 19: 1896–1902.

[16] Feng H, Cui Y, Liu J, Liu M, Zhou W, Yan Z, *et al*. Effects of 3-Methyladenine on Microglia Autophagy and Neuronal Apoptosis After Radiation-Induced Brain Injury. Dose-response: a Publication of International Hormesis Society. 2022; 20: 15593258221100593.

[17] Meshkini A, Ghorbani Haghjo A, Hasanpour Segherlou Z, Nouri-Vaskeh M. S100 Calcium-Binding Protein B and Glial Fibrillary Acidic Protein in Patients with Mild Traumatic Brain Injury. Bulletin of Emergency and Trauma. 2021; 9: 183–187.

[18] Morganti-Kossmann MC, Semple BD, Hellewell SC, Bye N, Ziebell JM. The complexity of neuroinflammation consequent to traumatic brain injury: from research evidence to potential treatments. Acta Neuropathologica. 2019; 137: 731–755.

[19] Liu XL, Sun DD, Zheng MT, Li XT, Niu HH, Zhang L, *et al*. Maraviroc promotes recovery from traumatic brain injury in mice by suppression of neuroinflammation and activation of neurotoxic reactive astrocytes. Neural Regeneration Research. 2023; 18: 141–149.

[20] Feng X, Zhan F, Luo D, Hu J, Wei G, Hua F, *et al*. LncRNA 4344 promotes NLRP3-related neuroinflammation and cognitive impairment by targeting miR-138-5p. Brain, Behavior, and Immunity. 2021; 98: 283–298.

[21] Xiao Q, Kang Z, Liu C, Tang B. *Panax notoginseng* Saponins Attenuate Cerebral Ischemia-Reperfusion Injury via Mitophagy-Induced Inhibition of NLRP3 Inflammasome in Rats. Frontiers in Bioscience (Landmark Edition). 2022; 27: 300.

[22] Ren H, Kong Y, Liu Z, Zang D, Yang X, Wood K, *et al*. Selective NLRP3 (Pyrin Domain-Containing Protein 3) Inflammasome Inhibitor Reduces Brain Injury After Intracerebral Hemorrhage. Stroke. 2018; 49: 184–192.

[23] Ismail H, Shakkour Z, Tabet M, Abdelhady S, Kobaisi A, Abedi R, *et al*. Traumatic Brain Injury: Oxidative Stress and Novel Anti-Oxidants Such as Mitoquinone and Edaravone. Antioxidants (Basel, Switzerland). 2020; 9: 943.

[24] Cheng DW, Yue YF, Chen CX, Hu YD, Tang Q, Xie M, *et al*. Emodin alleviates arthritis pain through reducing spinal inflammation and oxidative stress. Molecular Pain. 2022; 18: 17448069221146398.

[25] Lee EH, Baek SY, Park JY, Kim YW. Emodin in *Rheum undulatum* inhibits oxidative stress in the liver via AMPK with Hippo/Yap signalling pathway. Pharmaceutical Biology. 2020; 58: 333–341.

[26] Tan Z, Chen L, Ren Y, Jiang X, Gao W. Neuroprotective effects of FK866 against traumatic brain injury: Involvement of p38/ERK pathway. Annals of Clinical and Translational Neurology. 2020; 7: 742–756.

[27] Li XW, He RZ, Li Y, Ruan ZF. Tizoxanide mitigates inflammatory response in LPS-induced neuroinflammation in microglia via restraining p38/MAPK pathway. European Review for Medical and Pharmacological Sciences. 2020; 24: 6446–6454.